Raman Spectroscopy as a Probe of Low-Temperature Ionic Speciation in Nitric and Sulfuric Acid Stratospheric Mimic Systems

Nicholas Minogue, Eoin Riordan, and John R. Sodeau*

Department of Chemistry, University College Cork, Cork, Ireland

Received: July 29, 2002; In Final Form: December 31, 2002

The Raman spectroscopy technique has been employed to probe, as a function of temperature, the ionic and molecular speciation within the aqueous phase for systems of potential relevance to stratospheric chemistry. The systems studied, over the temperature range 200−300 K, were (i) binary HNO_3:H_2O and H_2SO_4:H_2O mixtures and (ii) ternary HNO_3:H_2SO_4:H_2O (NSW) mixtures. The contributions of the concentration coefficient, Q_m, to the equilibrium dissociation constants were assessed from the spectroscopic data. It was observed that speciation within the binary acid systems shifts toward the ionized form as temperature and concentration decrease because of increasing proton stabilization. The ternary NSW acid displays some similar properties to the binary counterparts, though a dominance of $SO_4^{2-}{}_{aq}$ over $NO_3^{-}{}_{aq}$ ions in the competition for protons is observed. This effect leads to the HSO_4^- ion becoming the principal associated acid form and its presence is found to determine the behavior of the NSW systems at all studied concentrations. The frozen acids are observed to be totally ionized, and detailed thermodynamic measurements of the freezing solutions suggest that homogeneous freezing will not occur at temperatures and concentrations for which associated species proliferate. It was found that the onset of freezing could be monitored spectrally by observation of an increasing scatter intensity maximizing at 300 cm^{-1}. Observation of this phenomenon therefore provided an indirect method of determining the temperature at which the solid-phase began to grow.

Introduction

The significance of sulfuric and nitric acids to both the formation and composition of stratospheric particles/droplets and their initiating role in ozone depletion mechanisms is well established.[1] However, the atmospheric form in which they exist has been the subject of much debate over the last fifteen years. Many recent observations suggest sulfuric acid aerosols and polar stratospheric clouds (PSCs) may remain liquid through supercooling to the lowest possible stratospheric temperatures. In contrast, several field measurements show the common occurrence of various crystalline hydrates of nitric and sulfuric acid above the frost point.[2−4] Hence stratospheric sulfate aerosols (SSA) are thought to be the precursors to polar PSC formation. As the temperature decreases, the sulfuric acid core deliquesces water and nitric acid vapor, forming a liquid ternary solution. Thermodynamic models have shown that these liquid particles will predominate even when the condensation nuclei are already solid crystalline sulfuric acid tetrahydrate (SAT) particles. Under conditions prevalent in the polar stratosphere, SAT deliquesces in the presence of nitric acid and water vapor, setting up a solid SAT−ternary liquid equilibrium. Sufficient condensation can force the particle into a completely ternary solution. Subsequent uptake of HNO_3 and H_2O is rapid over the temperature drop from 192 to 190 K, just above the frost point, such that the volume of PSC particles increases approximately 15-fold.[5−8] The existence of such surfaces, capable of affecting both atmospheric chemical composition and climate change, has therefore provoked much field and laboratory interest.

Recent campaign observations and associated modeling studies have focused attention upon the combined effects of global warming in the troposphere, and ozone depletion in the Arctic stratosphere. For example, the THESEO2000 project reported 60% ozone depletion at 18 km, between early January and late March of 2000, one of the most substantial ozone depletion events ever recorded in the region.[9] Furthermore, recent measurements of decreasing temperatures in the upper atmosphere may also provide the strongest indicators, so far obtained, of one real impact of the Greenhouse Effect. Hence, increased temperatures in the troposphere cause damping of Lee waves, thereby limiting their disruptive effect on the Arctic vortex. The effect leads subsequently to the observed "cooling" of the stratosphere.

Also, on the evidence of modeling studies, it has been proposed that tropospheric warming will lead to increased stratosphere−troposphere exchange, and a considerable increase in stratospheric water vapor concentrations.[10] The formation of increasing amounts of cold water−ice particles, i.e., PSC-type surfaces, may therefore be expected. Due to the established role of PSCs in the heterogeneous catalysis of chlorine-containing compounds in the stratosphere, there is clearly a need to understand their detailed physicochemical properties. To date there is little information available regarding the complex effects associated with changing PSC composition and temperature as a function of ionic content within the aqueous phase. This knowledge is important because the effects of speciation upon phase changes are fundamental to our ability to predict the chemical role of PSCs in a changing stratospheric environment.

The consensus of opinion regarding the phase condition of PSCs favors the existence of so-called "supercooled ternary solutions" under stratospheric conditions. This opinion has largely been based upon the thermodynamic models of Koop

10.1021/jp021746h CCC: $25.00 © 2003 American Chemical Society
Published on Web 05/08/2003

and Carslaw et al.[6−8] These suggest that sulfuric acid hydrates deliquesce in the presence of nitric acid and water vapor as the temperature decreases, thus forcing the aerosol into the aqueous phase. In fact, it has been reported that the phase of sulfuric acid is paramount. Nitric acid hydrates may form and coexist in ternary solutions, though the same is not true for sulfuric acid. For liquid aerosols to prevail, it is essential that sulfuric acid remains in the aqueous phase. The formation of sulfuric acid hydrates is only possible via heterogeneous nucleation within ice particles. Most of the predictions have been corroborated by laboratory experiments centered on the determination of homogeneous nucleation rates. Sulfate aerosols can be supercooled to temperatures well below those of stratospheric relevance, without the formation of crystalline hydrates, because freezing mechanisms are kinetically inhibited.[11−13] Indeed, contrary to earlier experimental reports,[14−16] it has been suggested that uptake of nitric acid into stratospheric aerosols occurs without freezing.[13,17]

Collection of PSC particles has proved exceptionally difficult because the complex phase relationships between liquid and crystalline particles demand intricate in situ analysis. However, a recent field experiment has shown it possible to assess chemical composition. These balloon-borne particle analysis measurements have observed Lee wave formed PSC particles with H_2O:HNO_3 ratios above 10, in agreement with ternary solution theories, rather than those centered on solid hydrates.[18]

To date spectroscopic studies of ternary solutions implicated in atmospheric heterogeneous chemistry have largely centered on IR investigations of thin-film "PSC mimics" under high vacuum conditions.[11,19−21] The spectra of different hydrates of nitric and sulfuric acid have been characterized by such methods, though there is still some debate concerning correct spectral assignments.[22] Some of the problems, which arise using such methods, originate with the broad IR bands exhibited by water. IR spectroscopic methods have also been used to study the vapors produced above ternary solutions, to elucidate possible reaction schemes for radical regeneration from stable chlorine species.[23,24] Most other studies have centered on the solubility and uptake by inorganic species in ternary solutions.[25−29]

Raman spectroscopy has rarely been used to investigate ionic speciation within ternary $H_2SO_4/HNO_3/H_2O$ (NSW) solutions. However, owing to the industrial importance of highly concentrated ternary solutions in the nitration of organic compounds, the formation of the nitrosonium ion, NO_2^+, has been studied using Raman spectroscopy.[30] Edwards et al. calculate a formation enthalpy for NO_2^+ of -25 kJ mol^{-1}, as determined from a van't Hoff plot over the temperature range 293−313 K. They neglected the role of activity in the equilibrium, so that the values of K_d they determine are actually those of the concentration quotient, Q_m.[31,32] There appear to be no reported Raman studies of ternary NSW solutions either at low temperatures or at lower concentrations. Therefore the major aim of this work is to provide such spectroscopic data to calculate thermodynamic parameters for the ionic dissociation of sulfuric and nitric acids under PSC-relevant conditions. The findings may then be utilized in appropriate atmospheric science model calculations of the system.

Experimental Section

An Ocean Optics R2000 Raman spectroscopic system[33] was employed for collection of in vitro Raman spectra. In this instrument a 500 mW, 785 nm diode laser delivers coherent radiation to the sample via a 400 nm diameter silica fiber optic probe. Scattered radiation is collected by a Gaser steered optical fiber[34] and returned through a filter to a dispersive spectrometer with no moving parts. A 1200 mm^{-1} blazed grating casts the spectrum across a 2048 element charge coupled device array. Spectra with resolution 16 cm^{-1} are collected over 4−60000 ms integration intervals, averaged and background corrected using a PC. The sample, contained in a round-bottomed vessel (to minimize laser reflections), was left open to the atmosphere in the laboratory (although during cooling, the flask was stoppered). It was cooled by an alcohol bath that was housed in a Thermos dewar flask and cooled between 303 and 200 K by a Neslab CC100 Cryocool refrigerator probe. The temperature of the sample was measured to 0.1 K resolution using a K-type thermocouple and monitored by a Hanna Instruments 93531 microprocessor-based thermometer.

Quantitative calibration of the system was performed for each analyte of interest, using sodium and ammonium sulfate, sodium bisulfate, and sodium nitrate solutions. The limits of quantitative detection were 0.001 mol dm^{-3} for sulfate and 0.01 mol dm^{-3} for nitrate ions. Overlapping peaks were resolved using Galactic PeakSolve. Quantitative linearity of the Raman response was attained for all these samples at both high and low concentrations with no significant deviation of the correlation with concentration.

TABLE 1: Raman Active Nitric Acid Vibrational Modes[30]

HNO_3	C_s	C_{2v}	wavenumber/ cm^{-1}
ν O−H	A′		
ν_{as} NO_2	A′	B_1	1673
$2 \times \delta$ out-of-plane	A′	A_1	1558
δ N−O−H	A′		
ν_s NO_2	A′	A_1	1304
ν N−(OH)	A′	A_1	955
δ out-of-plane	A″	B_2	
δ O−N−$O_{(scissors)}$	A′	A_1	688
δ O−N−$O_{(rock)}$	A′	B_1	640
δ $OH_{(torsion)}$	A″		

TABLE 2: Raman Active Nitrate Ion Vibrational Modes[30]

NO_3^-	D_{3h}	wavenumber/ cm^{-1}
$2 \times \delta$ out-of-plane	A′	1648
ν_{3as} NO_3	E′	1430
ν_{1s} NO_3	A′	1046
δ_2 out-of-plane	A″	
δ_4 O−N−O	E′	720

Results and Discussion

Nitric Acid: Concentration and Temperature Effects. The effect of increasing the nitric acid concentration is primarily to change its degree of ionization and solvation. Eventually, the system is transformed from one that is completely ionic in nature to one where appreciable amounts of both the molecular and ionic species are present. The Raman active bands with their assignments are shown in Tables 1 and 2 for nitric acid and the nitrate ion, respectively.

The Raman bands of molecular nitric acid, present at a 1:3 ratio of HNO_3:H_2O, are clearly diminished in intensity for the 1:10 and 1:20 solutions and suggest that ionization is almost complete at the latter concentrations. The results obtained at 298 K are summarized in Figure 1.

The temperature dependence of ionic speciation for nitric acid was measured at 1:3, 1:10, and 1:20 molar ratio concentrations of nitric acid. As described by Ratcliffe and Irish,[35] the

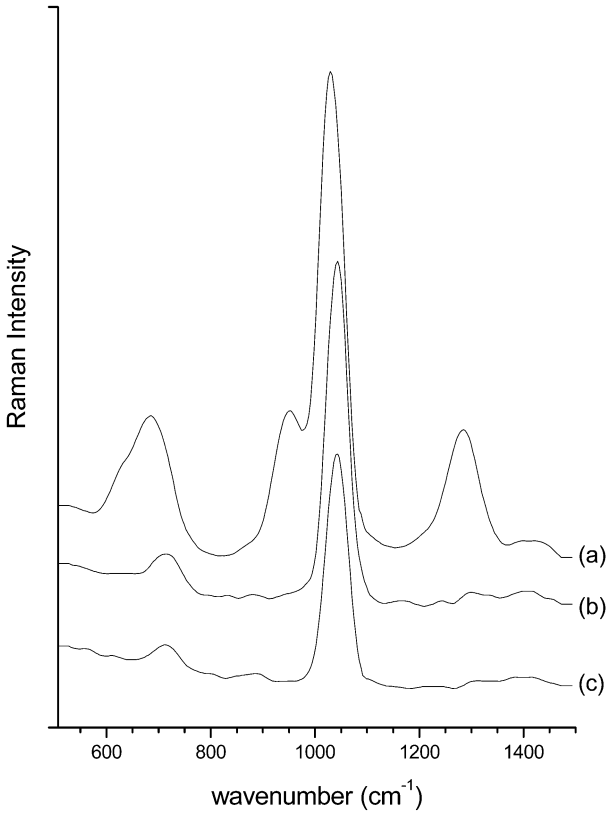

Figure 1. Raman spectra of nitric acid−water mixtures at ratios of (a) 1:3, (b) 1:10, and (c) 1:20, obtained at 298 K.

TABLE 3: Measured Degree of Dissociation (α) Values at Different Molar Ratios Nitric Acid: Water

T/K	1:3	1:10	1:20	1:5[a]
298	0.51	0.77	0.91	0.63
293	0.54	0.78	0.93	
288	0.56	0.81	0.95	
278	0.60	0.85	0.98	
268	0.65	0.90		
258	0.69	0.94	0.94	
248	0.73			

[a] Values recorded by Young et al.[36]

dissociation constant, K_d, can be deconvoluted into a concentration component, Q_m, and an activity component, Q_γ,

$$K_d = Q_m Q_\gamma$$

$$= \frac{\alpha^2 m}{1-\alpha} Q_\gamma = \frac{(m_{NO_3^-})^2}{m_{HNO_3}} Q_\gamma$$

where α is the degree of dissociation,

$$\alpha = \frac{m_{NO_3^-}}{m}$$

and m is the total amount of nitric acid and nitrate ion in solution ($m_{HNO_3} + m_{NO_3^-}$).

The measurements obtained in this work for monitoring the change in speciation of the nitric acid system with 1:3, 1:10, and 1:20 ratios at temperatures between 240 and 300 K are shown in Table 3. Concentrations of nitrate ion, with an error limit of 0.5%, were evaluated by use of a NO_3^- calibration plot and those of nitric acid, from the relationship, $m_{HNO_3} = m - m_{NO_3}$.

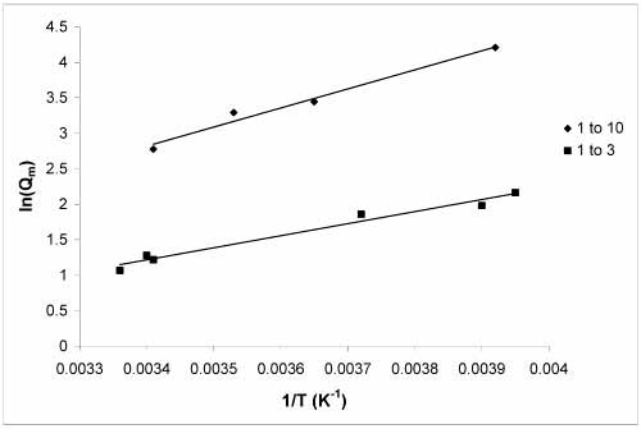

Figure 2. van't Hoff plot for 1:10 HNO_3:H_2O ($\Delta H = -22.8$ kJ mol^{-1}, $\Delta S = -54.6$ J mol^{-1} K^{-1}) and 1:3 HNO_3:H_2O ($\Delta H = -14.3$ kJ mol^{-1}, $\Delta S = -38.7$ J mol^{-1} K^{-1}) solutions.

Also included is a comparison value for α obtained using Raman spectroscopy by Young et al.[36] for a 1:5 ratio mixture at 298 K. It lies, appropriately, between the independently measured values for 1:3 and 1:10 ratios.

The determination of K_d over a range of temperatures enables, by use of the van't Hoff relationship, evaluations of (i) the enthalpy of the dissociation step, ΔH_d, and (ii) the entropy of the dissociation reaction, ΔS_d.

Plots of ln Q_m against $1/T$ at 1:3 and 1:10 ratios are shown in Figure 2. As indicated in the figure, the measurements lead to different values of ΔH (−22.8 kJ mol^{-1}/−14.3 kJ mol^{-1}) and ΔS (−54.6 J mol^{-1} K^{-1}/−38.7 J mol^{-1} K^{-1}), respectively. The estimated errors from this graphical treatment are 1−2% for the enthalpy values and 2−4% for the entropy counterparts. The overall effect is similar to that noted by Dawson et al. in their studies of ammonium bisulfate and is further discussed toward the end of this text.[37]

Because of the major role of nitric acid trihydrate (NAT) in laboratory studies of polar stratospheric cloud mimics, the effects of freezing on 1:3 nitric acid/water systems were studied in greater depth. Figure 3 shows the Raman spectra obtained for such mixtures cooled to 253, 241, and 227 K. Complete ionization to the nitrate ion is effected between the latter two temperatures, as indicated in Figure 3 and Table 1.

Analysis of the 1:3 HNO_3:H_2O system *during* freezing was also carried out by continuously collecting spectra throughout the cooling process. Five such time-dependent spectra, are shown in Figure 4. The solution was supercooled to 228 K over a period of 131 min; at this point the temperature was observed to increase to 254.4 K within 2 min. The system remained at this temperature for a considerable period of time (150 min), as indicated in Figure 4, despite being constantly cooled by the alcohol bath, which was held at 228 K. The two limiting temperatures correspond to the eutectic, T_e, and liquidus, T_l, values.[38] The spectra demonstrate the presence of molecular nitric acid in the solution (955 and 1304 cm^{-1}) right up to the onset of freezing, beginning after 141 min.

The spectroscopic and thermochemical observations indicate that a considerable re-organization of the liquid phase takes place upon the freezing of a 1:3 molar ratio nitric acid solution. It is probable that this change reflects the formation of crystalline NAT because the most stable structure of the crystalline form requires the ionization of HNO_3 to the more symmetrical NO_3^- ion. This stability is evidenced by the absence of a measurable

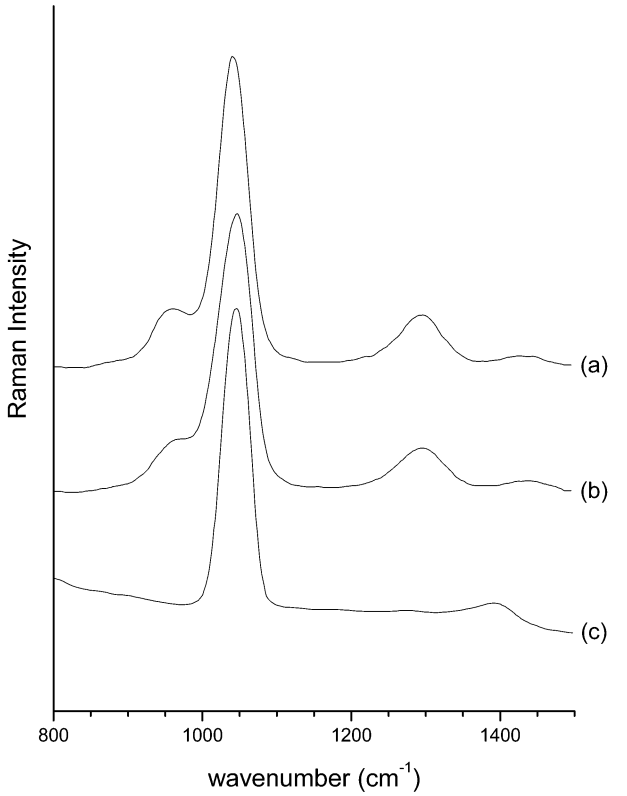

Figure 3. Offset Raman spectra recorded during the freezing of 1:3 HNO_3:H_2O sample: (a) 253 K, (b) 241 K, and (c) 227 K.

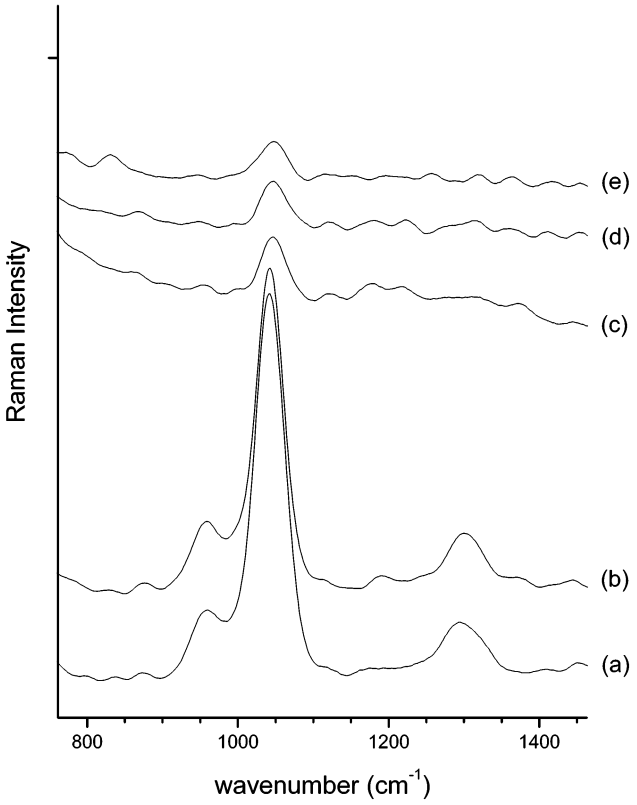

Figure 4. 1:3 HNO_3:H_2O mixture cooled for (a) 131, (b) 134, (c) 141, (d) 151, and (e) 290 min.

glass transition temperature, which usually corresponds to the re-organization of disordered water molecules in frozen solutions.[39]

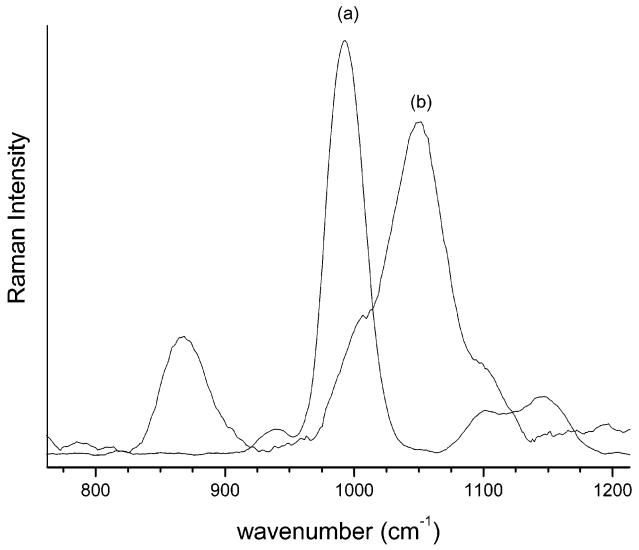

Figure 5. Raman spectra of (a) sodium sulfate and (b) sodium bisulfate salts.

TABLE 4: Raman Active Bisulfate Ion Vibrational Modes[32]

H_2SO_4	C_s	C_{3v}	wavenumber/ cm^{-1}
ν O−H	A′		3510
ν_{as} SO_3	A′	E	1191
ν_s SO_3	A′	A_1	1050
δ S−O−H	A′		1034
ν_s S−(OH)	A′	A_1	899
δ SO_3	A′	A_1	610[a]
ρ_w SO_3	A″	B_2	589[a]
ρ_r SO_3	A′	A_1	576[a]
δ_s O−S−OH	A′	E	447[a]
δ_{as} O−S−OH	A″		418[a]
τ OH	A″		407[a]

[a] These bands are obscured in the aqueous phase, by overlap with other species. Values given are for crystalline NH_4HSO_4.

TABLE 5: Raman Active Sulfate Ion Vibrational Modes[32]

SO_4^{2-}	D_{3h}	wavenumber/ cm^{-1}
ν_1 SO_4	A′	981
ν_2 SO_4	E′	451
ν_3 SO_4	T_1	1104
ν_4 SO_4	T_1	613

The amount of energy that had to be removed from the above system to allow crystallization is clearly important in the context of PSC formation, as it implies that long periods of supercooling may be required to enable solid NAT particles to form.

Sulfuric Acid: Concentration and Temperature Effects. Like the nitric acid system, the main effect of increasing the concentration of aqueous sulfuric acid is to change the speciation to less charged species; in this case from sulfate ions to bisulfate ions and eventually to molecular sulfuric acid. The values and assignments of the Raman active bands for sulfate and bisulfate ions are given in Tables 4 and 5, respectively. To corroborate the assignments, the spectra of pure sulfate and bisulfate (sodium) salts, recorded using the R2000 spectrometer, are shown in Figure 5. The vibrational modes used for the quantitative analyses performed in this work are observed at 980 cm^{-1} for the sulfate ion, 1050 and 899 cm^{-1} for the bisulfate ion and 1170 cm^{-1} for molecular sulfuric acid.

As expected, molecular sulfuric acid is visible only at the highest ratios, i.e., 1:<1 H_2SO_4:H_2O. In contrast, the bisulfate ion was always measured to be present in room temperature

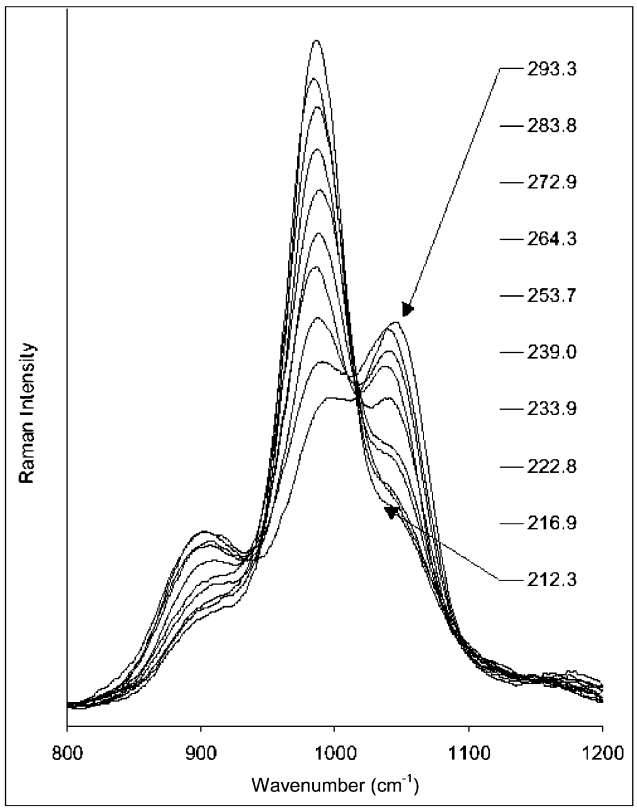

Figure 6. Raman spectra of 1:10 H_2SO_4:H_2O at various stages of the cooling process.

TABLE 6: van't Hoff Plot Data for 1:4, 1:10, and 1:20 H_2SO_4:H_2O Solutions

molar ratio H_2SO_4:H_2O	ΔH°_m/kJ mol^{-1}	ΔS°_m/J mol^{-1} K^{-1}
1:4	−13.2	−42.3
1:10	−24.7	−82.1
1:20	−42.0	−145

solutions. Thus, due to the importance of the bisulfate/sulfate equilibrium to aqueous atmospheric chemistry, its dependence on temperature, particularly upon supercooling was investigated more quantitatively.

Figure 6 shows the effect of temperature on the measured Raman spectra (labeled with their Kelvin values) of a 1:10 molar ratio sulfuric acid solution. It is clear from the results that as the temperature decreases, speciation shifts from bisulfate to sulfate ions. The solution remains in the aqueous phase even at 212 K. A similar set of data is obtained for 1:20 molar ratio sulfuric acid though the solution becomes frozen at 222 K. At both concentrations the bisulfate ion is clearly present at ambient temperatures. Tomikawa and Kanno[35] have measured the Raman spectra of sulfuric acid as a function of temperature and note the exponential increase of the ratios of sulfate to bisulfate intensity with decreasing temperature. However, they did not make any quantitative assessment of the system other than to note the total ionization to sulfate in the glassy aqueous solutions up to 60 wt % concentrations.

As discussed above, the relationship between Q_m and temperature can be investigated by use of a van't Hoff analysis. It was done so in this study for 1:4, 1:10, and 1:20 H_2SO_4:H_2O ratio solutions. The results are listed in Table 6 and show distinct trends. The enthalpy trend is one in which increasingly exothermic values of ΔH°_m are measured as a function of the increasing availability of the solvent. This behavior was similarly observed with the nitric acid systems. The entropy values for the dissociation reaction also become increasingly negative with increasing dilution.

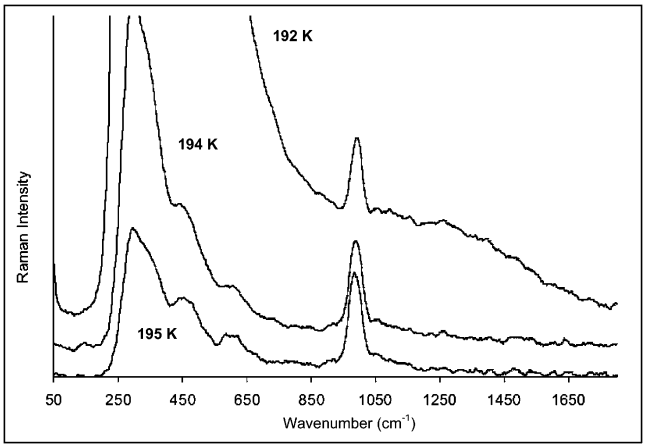

Figure 7. Raman spectra of the effect of freezing a 1:10 H_2SO_4:H_2O solution.

As mentioned above the total dissociation of sulfuric acid to sulfate ions in frozen glassy solutions of sulfuric acid has been reported by Kanno et al. for concentrations up to 60 wt % sulfuric acid (∼1:4 H_2SO_4:H_2O).[40,41] Figure 7 shows Raman spectra obtained for 1:10 H_2SO_4:H_2O ratio mixtures, cooled in liquid nitrogen, as the freezing process propagates through the sample. It is apparent that the solution is entirely dissociated to sulfate ions in each of these freezing solutions. The developing solid phase is indicated by an intensity increase in the underlying spectral feature maximizing at ∼300 cm^{-1}. This effect, observed below 195 K, is clearly associated with increased scatter from the generated solid phase and tracks with visual observation. Such results have not been explained before because none have been published hitherto using a fiber-optic Raman spectrometer. However, the obtained spectra can be interpreted in terms of a motion of the "freezing front" from the wall of the vessel toward the Raman spectrometer fiber-optic probe. Thus the Raman spectrum of the solution between the probe and the "freezing front" is observed as an overlay upon the intense scattering feature. Below 192 K, the sample becomes visibly frozen and the spectrum goes off-scale as a result of the degree of scattering originating from the solid phase.

Nitric Acid−Sulfuric Acid Mixtures: Concentration Dependence. Figure 8 shows Raman spectra obtained for ternary solutions of 1:1:10, 10:1:100, and 100:1:1000 HNO_3:H_2SO_4:H_2O (NSW) ratio mixtures at a temperature of 283 K. The concentration series may be considered as a set of representative mimics for the uptake and combination of nitric acid with water into a liquid sulfuric acid aerosol. It should be noted that the resolution afforded by the fiber optic Raman spectrometer was insufficient to prevent full spectral analysis of certain spectral features resulting from this complex ternary mixture due to band overlap. The difficulties were most apparent with the sulfate/bisulfate subsystem. Nonetheless, a number of semiquantitative observations can be made.

For example, and as expected, the Raman bands due to bisulfate and sulfate ions in the solutions clearly diminish as the mole fraction of sulfuric acid is reduced, e.g., ν_s S−(OH) for the bisulfate ion at 899 cm^{-1} and ν_1 SO_4^{2-} at 981 cm^{-1}. Furthermore, the presence of bisulfate in the NSW mixtures (as monitored by the ν_s S−(OH) mode) can be ascertained at all concentrations even down to the lowest ratio, 10:1:1000. However, it was also found that (i) the contribution of the symmetric −SO_3 stretching mode of HSO_4^- at 1050 cm^{-1} could

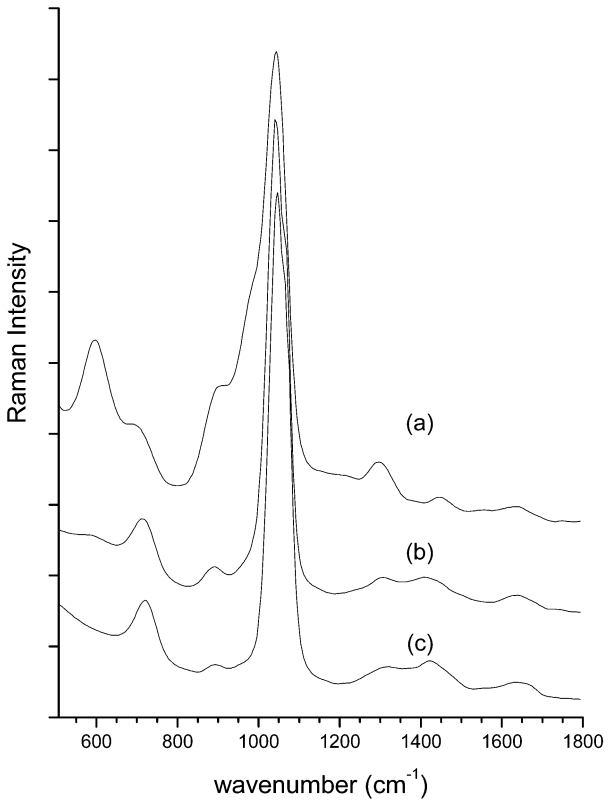

Figure 8. Offset Raman spectra of NSW solutions at ratios of (a) 1:1:10, (b) 10:1:100, and (c) 100:1:1000, at 283 K.

not be distinguished from that of the symmetric $-NO_3^-$ stretch at 1046 cm^{-1} and (ii) the 981 cm^{-1} peak originating with the SO_4^{2-} symmetric stretch was only discernible as a shoulder to the profile of the 1050/1046 cm^{-1} bands in the 1:1:10 HNO_3:H_2SO_4:H_2O spectrum. This feature was therefore more difficult to assess quantitatively at lower sulfuric acid concentrations.

In contrast, the ν_3 Raman band of the nitrate ion at 1430 cm^{-1} is observable in all solutions and increases in intensity with decreasing sulfuric acid content. Furthermore, the molecular nitric acid ν_1 mode observed at 1300 cm^{-1}, is clearly visible at a 1:1:10 NSW concentration ratio—even though molecular acid bands were barely discernible in the nitric acid binary system at this molar ratio. It measurably diminishes in intensity, as the mixture becomes more dilute in sulfuric acid.

Nitric Acid−Sulfuric Acid Mixtures: Temperature Dependence. In view of the above semiquantitative spectroscopic results on the concentration dependence of NSW speciation, the corresponding temperature dependencies were also investigated, because the addition of sulfuric acid to nitric acid solutions has been observed to depress the freezing point substantially. In fact, for solutions of nitric acid in the concentration range 0−33 wt %, the addition of 5 wt % sulfuric acid has been shown to lower the freezing point by up to 30 K.[43] This composition corresponds to a molar concentration ratio of up to 10:1:68 HNO_3:H_2SO_4:H_2O.

Although several experimental studies have investigated the nucleation statistics of the formation of solid hydrates from binary and ternary solutions, the effect of ionic speciation both at, and around, the freezing point has been neglected. Hence, a comparative Raman study for 1:1:10, 10:1:100, and 100:1:1000 NSW solutions between 222 and 303 K was made.

Spectroscopic observation of 1:1:10 NSW as it evolves with temperature show the expected increase in the degree of ionization as the temperature decreases. The Raman spectra obtained between 224 and 273 K are summarized in Figure 9.

Figure 10 shows the spectra of a 10:1:100 NSW mixture obtained at 303, 244, and 233 K. The sample remained liquid at all three temperatures. At 303 K, the presence of associated nitric acid is unequivocally observable through the ν_1 HNO_3 vibration at 1300 cm^{-1} (labeled N); the bisulfate band at 900 cm^{-1} is also apparent (labeled S) and the sulfate absorption at 980 cm^{-1} appears as a shoulder on the strong symmetric nitrate stretch at 1046 cm^{-1}. At 244 K, the molecular nitric acid becomes dissociated to nitrate ions (1430 cm^{-1}) whereas the bisulfate peak remains distinctly visible. At 233 K, the latter vanishes with concomitant intensity growth of the sulfate shoulder at 980 cm^{-1}.

Finally, temperature-dependent observations between 222 and 293 K were made for the 100:1:1000 NSW solution. Despite the similar mole fraction of nitric acid in the 10:1:100 NSW and the 100:1:1000 NSW solutions, the nitric acid appears almost totally dissociated at 293 K. The contrasting observation is probably caused by competition between the sulfate and nitrate subsystems for the acquisition of protons. At the lower mole fraction for sulfuric acid, the bisulfate component would normally be entirely dissociated into sulfate ions. However, in the presence of the nitric acid/nitrate ion equilibrium, association of the weaker acid occurs, resulting in the formation of bisulfate ions. As observed for the binary system with temperature decrease to 222 K, the bisulfate equilibrium shifts toward dissociated sulfate ions.

Nitric Acid−Sulfuric Acid Mixtures: Concentration-Temperature Dependence. Analysis of the 1300 cm^{-1} peak due to molecular nitric acid in a 1:1:10 NSW mixture produces a good linear correlation between HNO_3 concentration and temperature, as shown in Figure 11. The value of the molal scattering coefficient of HNO_3, J_{HNO_3}, can be extrapolated using values of HNO_3 concentration and Raman peak data measured in the binary acid mixtures study. The difference between the molarity of HNO_3 determined by this method and the total molarity of the nitric acid subsystem can therefore be evaluated to obtain α, the degree of dissociation in 1:1:10 NSW. Full dissociation is predicted at 171 K by this method.

The concentration contribution, Q_m, can also be calculated as discussed above for the binary mixtures and its relationship with temperature assessed. Figure 12 shows a van't Hoff plot of Q_m determined by this method. There are likely to be greater uncertainties in the determined values of Q_m for NSW than for the binary mixtures, because of the smaller peak intensities of the nitric acid band, which leads to error in the determination of J_{HNO_3}.

Implications of the Raman Studies to the Atmosphere. Early theories describing the nature of PSCs proposed a three-phase concept beginning with the formation of a sulfuric acid core followed by the condensation of nitric acid trihydrate (NAT). Then, at temperatures below the ice frost point, water was predicted to condense on the particle. These simple expectations have subsequently been developed into increasingly complex models to account for the weight of evidence supporting liquid ternary mixtures under certain conditions. However, little detailed physicochemical experimental information about the processes leading to freezing as a function of chemical composition is available.

The observed trends in the Raman spectroscopic data as a function of concentration are clearly indicative of strong interactions between the formed ionic species and the solvent. For example, as the acid concentrations decrease between 1:3

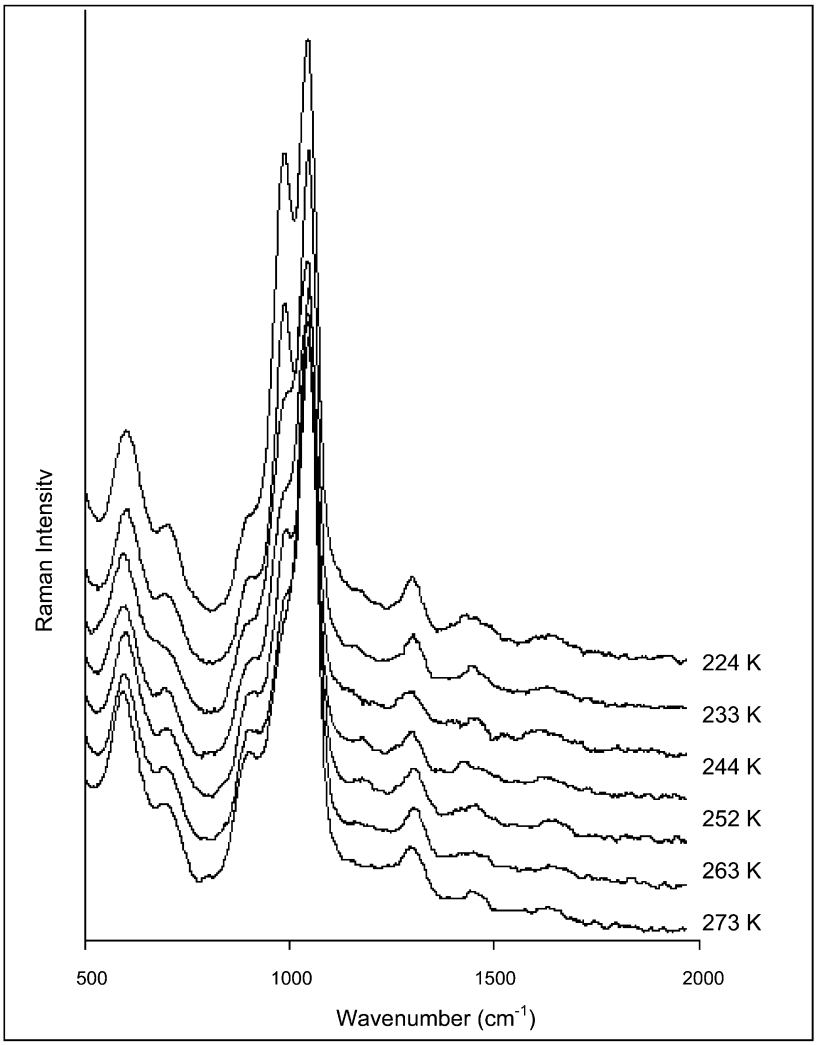

Figure 9. Raman spectra of a 1:1:10 NSW mixture as a function of temperature.

and 1:20 ratios, for both the nitric acid and sulfuric acid binary systems, the measured enthalpy becomes increasingly exothermic. This increase may be attributed to the increased stabilization of the ions by increasingly large hydration clusters, relative to the molecular species. (In related studies, successive hydration has been observed to lower the energy of the HCO_3^- ion by approximately 63 kJ mol^{-1} for each of the first five waters of hydration.)[44] Increasingly negative contributions to the reaction entropy with increasing dilution may also be interpreted in terms of the hydration of ionic species. Positive and negative ions surrounded by tightly bound water solvent molecules represent a state of increased order with respect to free water molecules. From the above spectro-thermodynamic measurements, the nitric acid and bisulfate equilibria may therefore be represented as

$$HNO_3 + nH_2O \rightarrow H_3O^+(H_2O)_a + NO_3^-(H_2O)_b \quad (1)$$

and

$$HSO_4^-(H_2O)_m + (n\text{-}m)H_2O \rightarrow H_3O^+(H_2O)_a + SO_4 = (H_2O)_b \quad (2)$$

where n is equal to $a + b$.

The temperature-dependent experimental studies described above constitute the first evaluation of the contributions of the concentration component, Q_m, to the dissociation constants of nitric and sulfuric acids using Raman spectroscopy. They have also provided valuable insight into the structure of the liquid phases for the two systems as they change with concentration, especially as they approach their respective freezing points. As either sample approaches the freezing point, complete ionization occurs just before freezing of the sample begins. In fact, the measurements clearly show that the solutions only freeze once total ionization of the materials in the aqueous phase has occurred.

In the freezing experiments for the 1:3 HNO_3:H_2O mixture, considerable amounts of energy were released by the system, which had to be removed in order for crystallization to progress. This energy originates with the exothermic dissociation of the nitric acid and must be released in order for solid, crystalline NAT to form. In the laboratory experiments the removal of this energy from the system required a considerable negative temperature gradient to be applied between the bath and the freezing solution: 30 K for 150 min. Such cooling rates are, of course, unlikely to be observed in the stratosphere.

For the ternary NSW solutions, the complete ionization of the nitric acid subsystem occurs before the complete ionization of bisulfate, regardless of the concentration ratios employed. This observation reflects the stronger acidity of nitric acid with respect to bisulfate and it is therefore proposed that the onset of freezing in NSW ternary solutions is controlled by the bisulfate equilibrium.

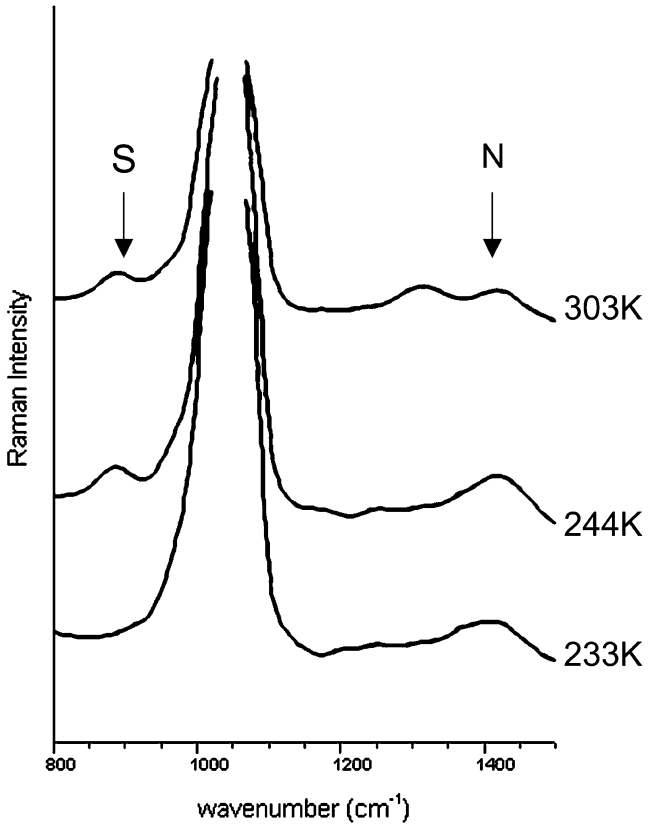

Figure 10. Raman spectra of 10:1:100 HNO_3:H_2SO_4:H_2O mixtures at three temperatures.

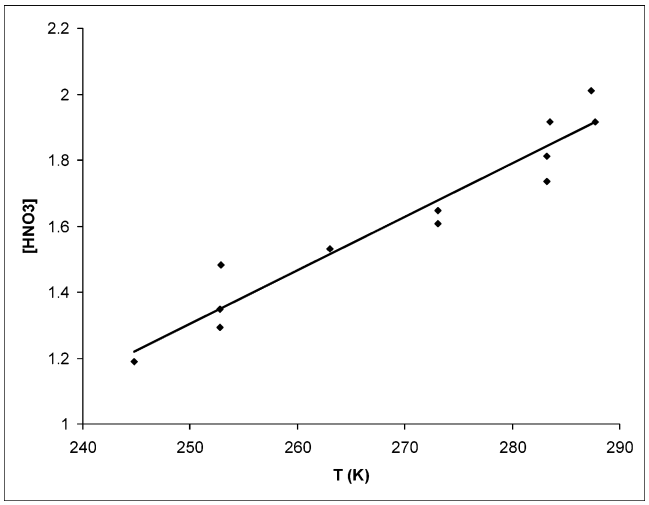

Figure 11. Concentration of nondissociated nitric acid in a 1:1:10 NSW ternary solution mixture: $[HNO_3] = 0.01662T - 2.849$, $R^2 = 0.932$, $\alpha = 1$ at 171 K.

The Raman spectra also show that the presence of bisulfate ions, even at concentrations below 1 in a 1000, hinders the formation of the solid phase. A number of other factors are also involved in this process because crystallization is a dynamic phenomenon with possible heterogeneous and homogeneous contributions. Initially, a small crystal "embryo" must form, from which the remaining crystals can nucleate. However "embryonic crystals" are energetically unfavorable as a result of the positive free energy associated with their interface to the liquid. This free energy barrier to nucleation must be overcome before freezing can commence. If insoluble foreign particles are present in the liquid, the "embryonic crystal" may be

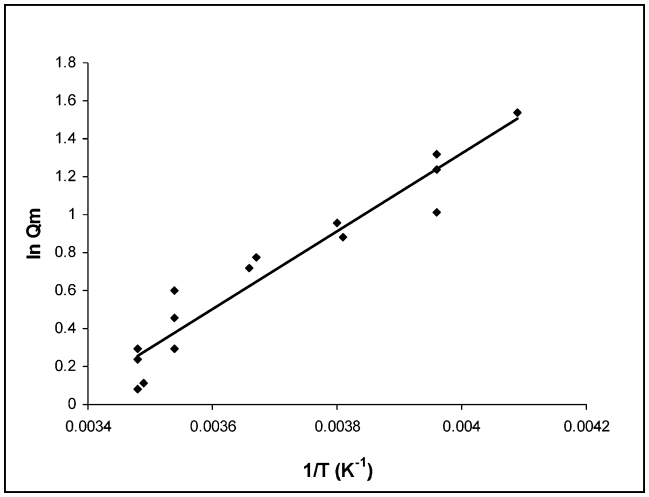

Figure 12. van't Hoff determination of nitric acid equilibrium in a 1:1:10 NSW ternary solution mixture: $\Delta H = -16.8$ kJ mol^{-1}, $\Delta S = -55.9$ J mol^{-1} K^{-1}.

stabilized, and freezing promoted: the heterogeneous nucleation process. In the absence of such surfaces, homogeneous nucleation must surmount the free energy barrier by utilizing thermal fluctuations in the liquid alone. In the case of binary and ternary acid solutions, the existence of nondissociated bisulfate ions and nitric acid further inhibits nucleation because their enthalpies of dissociation must also be accommodated before the lowest free energy system is reached, i.e., the totally ionized crystalline phase.

In terms of PSC-NAT and SSA-SAT field chemistry, the observed effects of temperature on ionic speciation suggest that total ionization is a prerequisite for solid hydrate formation. However, the measured enthalpies of dissociation are likely to inhibit the formation of crystalline hydrates under homogeneous freezing conditions. Laboratory studies have shown previously, and confirmed here, that heterogeneous freezing or rapid cooling rates may overcome the localized energy barriers to crystal growth (see, for example, ref 40). In these cases, it may be possible to deduce from the enthalpy results that lower hydrates, such as NAM/NAD or SAM/SAD, are more likely to form than higher hydrates under extreme dis-equilibrium conditions, because of the smaller energies needed to be removed from the system to totally ionize the acid. It has been proposed by Koop et al.[5] that the formation of nitric acid hydrates (NAX) can only occur once ice formation has begun. It is also suggested that NAX and ice may coexist with aqueous sulfuric acid, but that formation of sulfuric acid hydrates ensures the entire particle is in the solid phase.

In the context of these proposals, the significant role of the bisulfate equilibrium in phase changes of PSCs is affirmed. Thus the Raman spectroscopic findings explain why the formation of stable solid hydrates such as NAT and SAT from concentrated acid solutions under ambient stratospheric conditions is infeasible: the presence of nondissociated bisulfate ions prevent the process along with kinetic inhibition to nucleation.

Another important conclusion to be highlighted regarding the crystallization process is obtained by comparison of the binary sulfuric acid:water systems with their more diluted ternary counterparts. Hence a consequence of the presence of nitric acid is that water uptake by the ternary acid solutions is dramatically increased before attaining concentration ratios for which total ionization may prevail, thereby allowing the crystallization process to occur.

Finally, the possible coexistence of solid nitric acid hydrates and aqueous sulfuric acid in PSCs can be considered a reasonable hypothesis given that total ionization of the nitric acid system always occurs in the presence of nondissociated bisulfate ions.

References and Notes

(1) Finlayson-Pitts, B. J.; Pitts, J. N., Jr. *Chemistry of the Upper and Lower Atmosphere*; Academic Press: New York, 2000.

(2) Koop, T.; Luo, B.; Biermann, U. M.; Crutzen, P. J.; Peter, T. Freezing of $HNO_3/H_2SO_4/H_2O$ solutions at stratospheric temperatures: Nucleation statistics and experiments. *J. Phys. Chem. A* **1997**, *101*, 1117−1133.

(3) Peter, T. Microphysics and heterogeneous chemistry of polar stratospheric clouds. *Annu. Rev. Phys. Chem.* **1997**, *48*, 785−822.

(4) Reichardt, J.; Tsias, A.; Behrendt, A. Optical properties of PSC Ia − Enhanced at UV−visible wavelengths: Model and observations. *Geophys. Res. Lett.* **2000**, *27*, 201−204.

(5) Carslaw, K. S.; Clegg, S. L.; Brimblecombe, P. A Thermodynamic Model of the System $HCl-HNO_3-H_2SO_4-H_2O$, Including Solubilities of HBr, From <200 to 328 K. *J. Phys. Chem.* **1995**, *99*, 11557−11574.

(6) Carslaw, K. S.; Peter, T.; Clegg, S. L. Modeling the composition of liquid stratospheric aerosols. *Rev. Geophys.* **1997**, *35*, 125−154.

(7) Koop, T.; Carslaw, K. S. Melting of $H_2SO_4 \cdot 4H_2O$ particles upon cooling: Implications for polar stratospheric clouds. *Science* **1996**, *272*, 1638−1641.

(8) Koop, T.; Carslaw, K. S.; Peter, T. Thermodynamic stability and phase transitions of PSC particles. *Geophys. Res. Lett.* **1997**, *24*, 2199−2202.

(9) European Union Press Release. "Severe stratospheric ozone depletion in the Arctic" European Commission, 2000. http://www.nilu.no/projects/theseo2000/press-rel-000405.htm.

(10) Kirk-Davidoff, D. B.; Hintsa, E. J.; Anderson, J. G.; Keith, D. W. The effect of climate change on ozone depletion through changes in stratospheric water vapour. *Nature* **1999**, *402*, 399−401.

(11) Middlebrook, A. M.; Iraci, L. T.; McNeill, L. S.; Koehler, B. G.; Wilson, M. A.; Saastad, O. W.; Tolbert, M. A.; Hanson, D. R. Fourier Transform infrared studies of thin H_2SO_4/H_2O films − formation, water-uptake, and solid−liquid phase changes. *J. Geophys. Res.—Atmos.* **1993**, *98*, 20473−20481.

(12) Anthony, S. E.; Tisdale, R. T.; Disselkamp, R. S.; Tolbert, M. A.; Wilson, J. C. FT-IR studies of low-temperature sulfuric acid aerosols. *Geophys. Res. Lett.* **1995**, *22*, 1105−1108.

(13) Koop, T.; Luo, B.; Biermann, U. M.; Crutzen, P. J.; Peter, T. Freezing of $HNO_3/H_2SO_4/H_2O$ Solutions at Stratospheric Temperatures: Nucleation Statistics and Experiments. *J. Phys. Chem. A* **1997**, *101*, 1117−1133.

(14) Molina, M. J.; Zhang, R.; Wooldridge, P. J.; McMahon, J. R.; Kim, J. E.; Chang, H. Y.; Beyer, K. D. Physical chemistry of the $H_2SO_4/HNO_3/H_2O$ system − Implications for polar stratospheric clouds. *Science* **1993**, *261*, 1418−1423.

(15) Worsnop, D. R.; Zahniser, M. S.; Kolb, C. E.: Wofsy, S. C.; Fox, L. E. Vapor-pressures of $HNO_3/HCl/H_2O$ mixtures at stratospheric temperatures. *Abstr. Pap. Am. Chem. Soc.* **1990**, *200*, 29.

(16) Fox, L. E.; Worsnop, D. R.; Zahniser, M. S.; Wofsy, S. C. Metastable phases in polar stratospheric aerosols. *Science* **1995**, *267*, 351−355.

(17) Salcedo, D.; Molina, L. T.; Molina, M. J. Nucleation rates of nitric acid dihydrate in 1:2 HNO_3/H_2O solutions at stratospheric temperatures. *Geophys. Res. Lett.* **2000**, *27*, 193−196.

(18) Schreiner, J.; Voigt, C.; Kohlmann, A.; Arnold, F.; Mauersberger, K.; Larsen, N. Chemical analysis of polar stratospheric cloud particles. *Science* **1999**, *283*, 968−970.

(19) Horn, A. B.; Sully, K. J. ATR−IR spectroscopic studies of the formation of sulfuric acid and sulfuric acid monohydrate films. *Phys. Chem. Chem. Phys.* **1999**, *1*, 3801−3806.

(20) Koch, T. G.; Holmes, N. S.; Roddis, T. B.; Sodeau, J. R. Low-temperature reflection/absorption IR study of thin films of nitric acid hydrates and ammonium nitrate adsorbed on gold foil. *J. Chem. Soc., Faraday Trans.* **1996**, *92*, 4787−4792.

(21) Iraci, L. T.; Middlebrook, A. M.; Wilson, M. A.; Tolbert, M. A. Growth of nitric acid hydrates on thin sulfuric acid films. *Geophys. Res. Lett.* **1994**, *21*, 867−870.

(22) Nash, K. L.; Sully, J. K.; Horn, A. B. Infrared spectroscopic studies of the low-temperature interconversion of sulfuric acid hydrates. Submitted to *Phys. Chem. Chem. Phys.*

(23) Luick, T. J.; Heckert, R. W.; Schulz, K.; Disselkamp, R. S. Nitrosyl and nitryl chloride formation in $H_2SO_4/HNO_3/H_2O$/HCl solutions at 200 K. *J. Atmos. Chem.* **1999**, *32*, 315−325.

(24) Tolbert, M. A.; Rossi, M. J.; Golden, D. M. Heterogeneous interactions of chlorine nitrate, hydrogen chloride, and nitric acid with sulfuric acid surfaces at stratospheric temperatures. *Geophys. Res. Lett.* **1988**, *15*, 847−850.

(25) Elrod, M. J.; Koch, R. E.; Kim, J. E.; Molina, M. J. HCl vapour pressures and reaction probabilities for $ClONO_2$ + HCl on liquid $H_2SO_4-HNO_3-HCl-H_2O$ solutions. *Faraday Discuss.* **1995**, 269−278.

(26) Robinson, G. N.; Worsnop, D. R.; Jayne, J. T.; Kolb, C. E.; Davidovits, P. Heterogeneous uptake of $ClONO_2$ and N_2O_5 by sulfuric acid solutions. *J. Geophys. Res.—Atmos.* **1997**, *102*, 3583−3601.

(27) Hanson, D. R. Reaction of $ClONO_2$ with H_2O and HCl in sulfuric acid and $HNO_3/H_2SO_4/H_2O$ mixtures. *J. Phys. Chem. A* **1998**, *102*, 4794−4807.

(28) Zhang, R. Y.; Leu, M. T.; Molina, M. J. Formation of polar stratospheric clouds on preactivated background aerosols. *Geophys. Res. Lett.* **1996**, *23*, 1669−1672.

(29) Massucci, M.; Clegg, S. L.; Brimblecombe, P. Equilibrium vapor pressure of H_2O above aqueous H_2SO_4 at low temperature. *J. Chem. Eng. Data* **1996**, *41*, 765−778.

(30) Librovich, N. B.; Rassadin, B. V.; Medvetskaya, I. M.; Andreeva, L. R.; Vinnik, M. I. Raman spectra of nitric acid in aqueous sulfuric acid solutions. *Bull. Acad. Sci. USSR Div. Chem. Sci.* **1984**, *33*, 1401−1405.

(31) Edwards, H. G. M.; Turner, J. M. C.; Fawcett, V. Raman spectroscopic study of nitronium ion formation in mixtures of nitric acid, sulfuric acid and water. *J. Chem. Soc., Faraday Trans.* **1995**, *91*, 1439−1443.

(32) Edwards, H. G. M.; Fawcett, V. Quantitative raman spectroscopic studies of nitronium ion concentrations in mixtures of sulfuric and nitric acids. *J. Mol. Struct.* **1994**, *326*, 131−143.

(33) Ocean Optics Ltd. *Manufacturer's Website*, 2000, www.OceanOptics.com.

(34) Visonex Ltd. *Manufacturer's Website*, 2000, www.visionex.com.

(35) Ratcliffe, C. I.; Irish, D. E. Vibrational spectral studies of solutions at elevated temperatures and pressures 0.7. Raman spectra and dissociation of nitric acid. *Can. J. Chem.—Rev. Can. Chim.* **1985**, *63*, 3521−3525.

(36) Young, T. F.; Maranville, L. F.; Smith, H. M. In *The Structure of Electrolyte Solutions*; Hamer, W. J., Ed.; Wiley and Sons: New York, 1959; Chapter 4.

(37) Dawson, B. S. W.; Irish, D. E.; Toogood, G. E. Vibrational spectral studies of solutions at elevated temperatures and pressures. 8. A Raman spectral study of ammonium hydrogen sulfate solutions and the $HSO_4^- - SO_4^{2-}$ equilibrium. *J. Phys. Chem.* **1986**, *90*, 334−341.

(38) Satoh, K.; Kanno, H. Anomolous crystallisation behaviour in the glass forming composition region of the H_2O-HNO_3 system. *Bull. Chem. Soc. Jpn.* **1982**, *55*, 1645−1646.

(39) Fletcher, N. H. *The chemical physics of ice*; Cambridge University Press: Cambridge, U.K., 1970.

(40) Tomikawa, K.; Kanno, H. Raman study of sulfuric acid at low temperatures. *J. Phys. Chem. A* **1998**, *102*, 6082−6088.

(41) Kanno, H. Complete ionization of concentrated sulfuric acid at low temperatures. *Chem. Phys. Lett.* **1990**, *170*, 382−384.

(42) Horn, A. B. Vibrational assignments of H_3O^+. Personal communication.

(43) Chang, H. Y. A.; Koop, T.; Molina, L. T.; Molina, M. J. Phase transitions in emulsified HNO_3/H_2O and $HNO_3/H_2SO_4/H_2O$ solutions. *J. Phys. Chem. A* **1999**, *103*, 2673−2679.

(44) Yang, X.; Castleman, A. W. Chemistry of large hydrated anion clusters $X-(H_2O)_n$, $n = 0-59$ and X = OH, O, O_2, and O_3. 3. Reaction of SO_2. *J. Phys. Chem.* **1991**, *95*, 6182−6186.

(45) Bertram, A. K.; Dickens, D. B.; Sloan, J. J. Supercooling of type I polar stratospheric clouds: The freezing of submicron nitric acid aerosols having HNO_3 mole fractions <0.5. *J. Geophys. Res.* **2000**, *105*, 9283−9290.